Journal of Solid State Electrochemistry
https://doi.org/10.1007/s10008-024-06036-9

ORIGINAL PAPER

Role of electrode temperature in anodic growth of sulfuric acid alumina films

Boriana Tzaneva[1] · **Igor Vrublevsky**[2] · **Valentin Videkov**[1] · **Nikita Lushpa**[2]

Received: 30 June 2024 / Revised: 30 July 2024 / Accepted: 1 August 2024

Abstract

Studies of the self-organized growth of nanoporous anodic aluminum oxide (AAO) films and anodization parameters have been the subject of decades of research and various theories. At the same time, temperature, being one of the most important parameters in anodizing treatments of aluminum, has been investigated only as a function of electrolyte temperature. This paper presents the results of studying the growth kinetics and morphology of AAO formed by anodization processes in 1 M H_2SO_4 at different anode temperatures. The activation energy of ionic conductivity for AAO determined in this study was 0.41 eV for sulfuric acid, which was greater than the activation energy of 0.34 eV for oxalic acid. The effect of anode temperature on the pore diameter (d_{pore}) and the interpore distance (D_{inter}) was studied. It was demonstrated that in the temperature range from 10 to 40 °C, the d_{pore} and D_{inter} did not change with the anode temperature, with values equal to 12.5 ± 0.1 nm and 52.5 ± 0.2 nm, respectively. However, when the anode (aluminum) temperature was increased to 60 °C, the d_{pore} increased to 16 nm. The results obtained show that by increasing the temperature of the anode from 20 to 40 °C, it is possible to increase the ionic conductivity of AAO and thus achieve a greater than threefold increase in the the rate of AAO growth, without altering the porous morphology of the anodic films.

Keywords Anodic alumina · Sulfuric acid · Electrode temperature · Ionic conductivity · Activation energy

Introduction

Anodic aluminum oxide (AAO) is widely used for the production of nanoporous membranes with high structural perfection. The possibility of obtaining an ordered porous structure has driven the growth in the use of AAO for fabrication of nanostructures used in electronic, magnetic, and photonic devices and in various radioelectronics products [1–5]. The technology for producing nanoporous AAO is characterized by a high degree of control over its properties through appropriate selection of anodization parameters including composition and electrolyte temperature, anodizing voltage, current density, and anodization time [6–8]. The parameters of the porous structure of anodic films, such as pore diameter and interpore distance, can be controlled by varying the anodizing voltage [9, 10].

A critical parameter, in addition to anodizing voltage, that allows us to achieve control over the porous structure of AAO films is temperature [11, 12]. For example, an increase in electrolyte temperature has a noticeable effect on both the rate of aluminum anodization and the increase in the surface microrelief of porous anodic oxide films.

The influence of electrolyte temperature has been studied in many works [13–17]. However, the influence of another important parameter—anode (aluminum) temperature—on the growth of porous AAO is still poorly investigated. The results of such studies are of great value, since they provide information about the ion transfer processes in AAO. This is because the mass transfer caused by migration of Al^{3+} cations and O^{2-} anions under the effect of an electric field has a noticeable effect on the growth rate of AAO.

In order to provide precise temperature control for this kind of experiment, a thermoelectric Peltier device can be used. In [18], the influence of the aluminum substrate temperature was investigated with respect to the porous structure and thickness of anodic films formed in oxalic acid at a

✉ Igor Vrublevsky
vrublevsky@bsuir.edu.by

[1] Technical University of Sofia, St. Kl. Ohridski Blvd 8, 1000 Sofia, Bulgaria

[2] Belarussian State University of Informatics and Radioelectronics, P.Brovki 6, 220013 Minsk, Belarus

Published online: 19 August 2024

constant voltage. The results obtained using a solution-flow type microdroplet cell design showed that the pore diameter of AAO for anodized strips increased with increasing substrate temperature. In this case, the interpore distance in anodic films did not change. These results, however, have limited application due to the small volume of electrolyte used in the design of a solution-flow-type microdroplet cell for anodizing aluminum. In [19], the aluminum substrate temperature was controlled in the temperature range of 5–65 °C using a thermoelectric Peltier device. Porous AAO was formed at constant current in an aqueous solution of sulfuric acid with the addition of $Al_2(SO_4)_3$. However, the choice of aluminum anodizing modes at constant current does not allow one to evaluate the effect of the substrate temperature on the morphology of anodic films, which limits the value of such results.

We have previously studied the effect of anode temperature on the formation of porous AAO in oxalic acid [20]. The results confirmed that in order to obtain high growth rates while maintaining the quality and microstructure of the formed anodic films, a higher anode temperature can be used for the aluminum anodization process. The purpose of the present work was to study the effect of anode temperature on the growth rate and microstructure of porous AAO (interpore distance and pore diameter) and to determine the nature of ionic conductivity in AAO in the case of anodization of aluminum in sulfuric acid.

Experimental

High-purity aluminum foils (99.999% Al, Alfa Aesar) with thickness of 25 and 100 μm were used as starting material. Analytical-grade chemicals and distilled water were employed for the preparation of all experimental solutions.

The aluminum samples were first degreased in acetone. They were then pretreated in a hot solution of 1.5 M NaOH for 15 s, neutralized in 1.5 M HNO_3 for 2 min, and carefully rinsed in distilled water and dried with warm air.

AAO was formed by two-stage anodization of 25-μm-thick aluminum foil in 1.0 M sulfuric acid at an electrolyte temperature of 20 °C and voltage of 20 V. The first anodization was carried out on both sides of the samples at 20 V and at an electrolyte temperature of 20 °C for 30 min. After this operation, the porous Al_2O_3 layer was completely removed by dissolving it in a mixture of $H_3PO_4 + CrO_3$ at 75 °C for 2 h. The second anodization was carried out at a constant electrolyte temperature of 20 °C and anode temperature ranging from 5 to 70 °C until the aluminum was completely oxidized. The design of the electrochemical cell that was used is described in detail in our previous works [20, 21]. A polytetrafluoroethylene (PTFE) electrochemical cell, consisting of two main parts, was used to study the temperature effects and to control the anodization processes. The first part included an electrochemical cell with a tank for the electrolyte, and with a heat exchanger and electrolyte temperature control. The aluminum substrate under study was placed at the bottom, on the base of the electrochemical cell. The second part contained a heating module. A thermoelectric Peltier device was used to control the aluminum substrate temperature. The electrolyte temperature was kept constant using a cryostat and electrolyte stirring. It is known that the thermal conductivity of aluminum changes from 236 to 238 W/(K·m) when the temperature rises from 0 to 70 °C. On the other hand, the thermal conductivity of porous oxide layers obtained in a sulfuric acid solution stays in the range from 1.0 to 0.5 W/(K·m) when the temperature increases from 0 to 40 °C [22, 23], which is close to that of sulfuric acid solution (from 0.316 to 0.584 W/[K·m] for temperatures from 5 to 70 °C, respectively) [24]. The thermal resistance of aluminum oxide resulted in temperature gradients between the electrolyte and the aluminum. The temperature gradient, therefore, is mainly concentrated in the oxide layer. The value of this gradient depended on the heating power of the aluminum substrate, which was set by the thermoelectric Peltier device.

Single-sided anodization was carried out on an aluminum surface area of 2.54 cm^2 using a platinum cathode. A Voltcraft (Germany) DC power supply (40 V/5 A) was used for the anodization process. Transient currents during anodizing were measured and recorded on a computer in real time using a UNI-T UT71E digital multimeter with a data sampling rate of 60 points/min. After anodization, porous AAO films were thoroughly washed with distilled water and dried with warm air.

The nanoporous morphology of anodic films obtained at different anode temperatures was studied by scanning electron microscopy (SEM) using a LEO DSM 982 instrument (Germany). The pore size and interpore distance were determined from SEM images of the surface morphology of anodic films using ImageJ software.

Results and discussion

Effect of anode temperature on transient currents

Figure 1 shows a plot of the anodic current density versus Al anodization time for the range of anode temperature from 5 to 60 °C. Three stages of growth of anodic Al_2O_3 can be distinguished. The first stage lasts about 1 min and is associated with a sharp increase in current density until a stationary value is reached. For anode temperatures up to 40 °C, the current curves reveal a clearly defined plateau

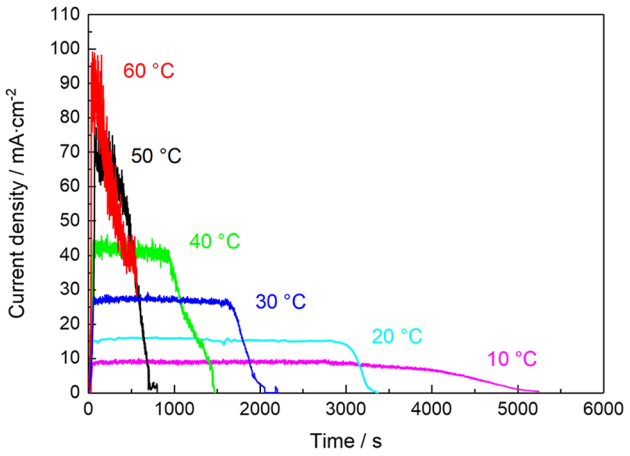

Fig. 1 Current transients for porous anodic alumina formation at different anode temperatures of 10–60 °C in a 1.0 M sulfuric acid solution (20 °C)

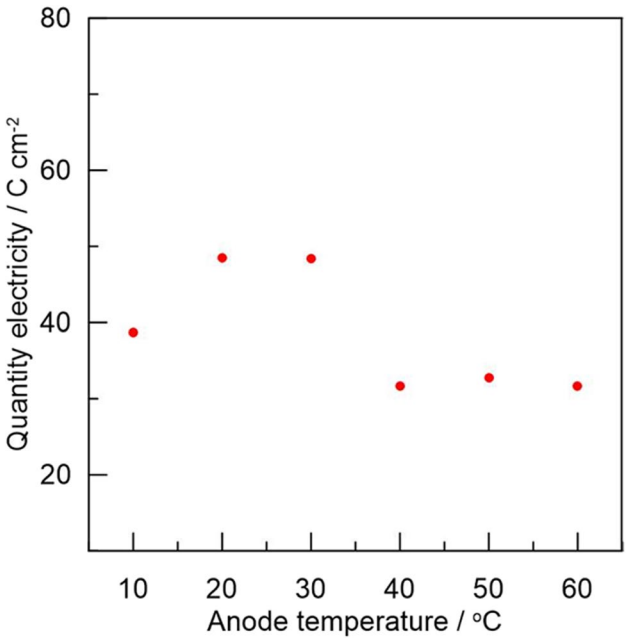

Fig. 2 The effect of anode temperature on specific quantity of electricity of oxide layer

(second stage), which is associated with the stationary growth of AAO.

With an increase in anode temperature from 10 to 60 °C, the anodic current density in the second stage increases by approximately one order of magnitude (from 9 to 95 mA·cm^{-2}), with a decrease in the duration of this stage. When the anode temperature is above 50 °C, the process accelerates and the aluminum foil is anodized in less than 5 min, and therefore no plateau is observed. For this reason, studies with anode temperatures of 60 and 70 °C were additionally repeated with aluminum foil of greater thickness.

It is worth mentioning that due to the presence of slight irregularities in the thickness, there are separate, thicker areas on aluminum foil that take longer to anodize. This results in a gradual decrease in the detected current during the third stage due to the progressively decreasing surface area of the aluminum at the final stage of the anodization process. The time for complete anodization of aluminum foil (the end of the third stage) is decreased 5.5-fold with an increase in anode temperature from 10 to 60 °C.

It is also important to evaluate the electrical power required for anodization of aluminum. Specifically, for complete anodization of aluminum with an area of 1 cm^2:

$$\int_0^t J(t)\mathrm{d}t, \mathrm{C}\cdot\mathrm{cm}^{-2} \tag{1}$$

where j is anodic current density and t is the time of complete anodization of aluminum. The electrical power is defined as the area under the J–t curve in Fig. 1. It is observed that Q passes through a maximum of about 50 C·cm^{-2} in the anode temperature range of 20–30 °C (Fig. 2).

According to Faraday's law of electrolysis, one can expect that oxidation of samples with equal amounts of aluminum would consume the same amount of electricity. Therefore, the higher values of Q at temperatures below 40 °C indicate that in addition to aluminum oxidation, a competitive reaction occurs. The most frequently discussed competing reaction during anodization is the oxygen evolution reaction [25]. Release of oxygen takes place according to the following reaction:

$$2\mathrm{H_2O} \rightarrow \mathrm{O_2} + 4\mathrm{H^+} + 4\mathrm{e^-} \tag{2}$$

This is unlikely during anodization of high-purity aluminum because electron transfer from the film/electrolyte interface to the metal through the high-resistance barrier layer is negligible [26]. On the other hand, at sufficiently high electric fields, O^{2-} ions of aluminum oxide can provide an alternative source of oxygen:

$$2\mathrm{O^{2-}} \rightarrow \mathrm{O_2} + 4\mathrm{e^-} \tag{3}$$

This reaction occurs at the metal/oxide interface and is more likely when metal impurities are present in anodizing aluminum or in the case of aluminum alloys [26, 27]. The reaction of oxygen release, however, has been proven to occur with pure aluminum as well, and is the basis of the oxygen bubble model for the formation of pores in AAO [28, 29].

It is also well known that high temperature favors the transfer of Al^{3+} to the oxide/electrolyte interface, and the

anodization rate increases [30]. When the temperature of the aluminum substrate is higher than 40 °C, as will be shown later in the paper, Al^{3+} ions will form at a higher rate than the rate of AAO growth. As a result, the oxygen released at the electrolyte/oxide interface will interact with Al^{3+} ions on the surface to form aluminum oxide. Therefore, for the electrochemical oxidation of aluminum in this case, a smaller quantity of electricity (Q) will be needed. This explains the decrease in Q at higher temperatures, where the efficiency of the anodization process approaches 100%.

Effect of anode temperature on ionic conductivity of anodic Al_2O_3

Figure 3 shows anodic current density (J_a) versus anode temperature (T_{anode}) plots for stage II. As can be seen, with increasing anode temperature, anodic current density increases exponentially. It is worth mentioning that anodic current during aluminum anodization is almost entirely ionic current. The conductivity of AAO in this case is, therefore, ionic in nature. The result of ion transfer under the effect of a strong electric field in anodic oxide, O^{2-} anions to the Al_2O_3/Al interface and Al^{3+} cations to the electrolyte/Al_2O_3 interface is the formation of new layers of aluminum oxide at these boundaries. Consequently, the electrochemical characteristics of such systems are determined primarily by the characteristics of ion transport. The temperature dependence of ionic conductivity has an Arrhenius character and is described by the following formula [31]:

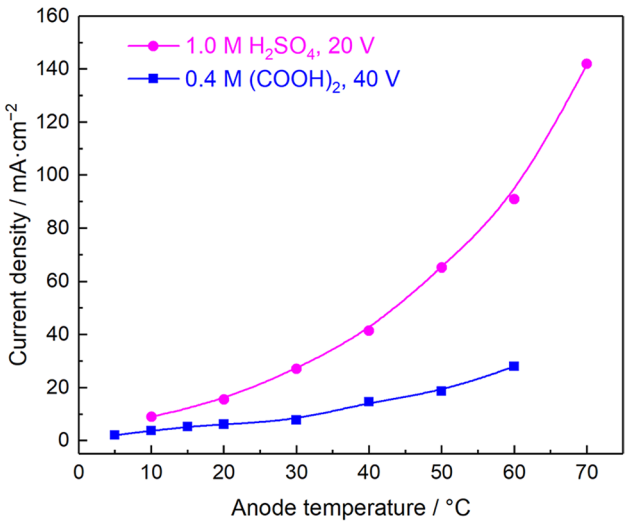

Fig. 3 The average current density during aluminum steady-state anodization at an electrolyte temperature of 20 °C in 1.0 M H_2SO_4 and in 0.4 M oxalic acid at 20 and 40 V, respectively, as a function of anode temperature

$$\sigma = \frac{\sigma_0}{T} exp\left(-\frac{E_a}{kT}\right) \tag{4}$$

where σ is ionic conductivity, E_a is the activation energy of ionic conductivity, T is the absolute temperature, and σ_0 is a constant.

The electrical conductivity of dielectrics depends on their chemical composition and structure and is determined by the migration of ions. The electrical conductivity of the dielectric σ is given by the expression

$$\sigma = cq\mu \tag{5}$$

where c is the concentration of mobile ions, q is the ionic charge, and μ is the ion mobility. The concentration c and mobility μ of ions depend on the temperature. Consequently, the electrical conductivity σ of the dielectric is a function of temperature. In general, the current density J_a is related to the conductivity σ in the dielectric by the following equation:

$$J_a = \sigma E \tag{6}$$

In the case of porous anodization of aluminum in potentiostatic mode, the electric field strength in the barrier layer of AAO remains constant. Therefore, it is possible to use the ionic current density J_a instead of conductivity σ in Eq. (4).

Plotted in Arrhenius coordinates, the ionic conductivity versus temperature curve has the form of a straight line (Fig. 4). The activation energy for ionic conductivity calculated for AAO formed in sulfuric acid is 0.41 eV. This value is in good agreement with the activation energy of 0.48 eV, which was obtained in [32] from the results of direct electrical measurements for AAO formed in sulfuric acid.

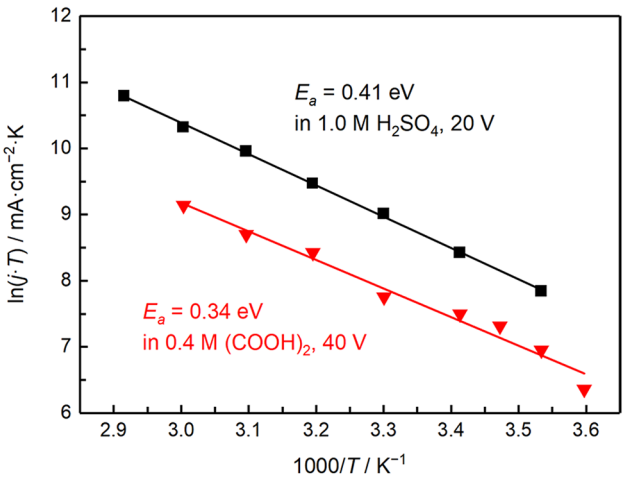

Fig. 4 Ionic conductivity of anodic aluminum oxide vs. anode temperature plotted in Arrhenius coordinates for sulfuric and oxalic acid

It is important to compare the results obtained for sulfuric acid with the same parameters for Al anodization in oxalic acid using the data from [20]. As can be seen in Fig. 4, the ionic conductivity versus temperature plot in Arrhenius coordinates has the same form. According to the graph, the activation energy of ionic conductivity for AAO in oxalic acid is 0.34 eV.

It is known that the activation energy of ionic conductivity for polycrystalline and amorphous dielectrics increases with deviations from stoichiometry. This is explained by the peculiarity of ion migration in a dielectric in the presence of defects such as impurities. Due to their small radii, the cations are more mobile than the anions. The incorporation of anionic impurities with a radius larger than the radius of oxygen ions into the structure of AAO leads to a change in the potential interaction energy of cations and, as a consequence, to an increase in the activation energy of ionic conductivity. The lower activation energy of ionic conductivity in the case of oxalic acid relative to sulfuric acid may indicate that the composition of AAO obtained in oxalic acid contains a smaller amount of electrolyte anion residues (impurities).

This is in good agreement with the data on the percentage of anions incorporated into the porous oxide layer of Al_2O_3 for sulfuric acid (10–13%) and oxalic acid (2–3%) [33]. It is also evidenced by the formulas calculated in [34] for the composition of AAO, taking into account the following content of impurities: for sulfuric acid, $(Al_2O_{2.77})_{100}(SO_4)_{19}(OH)_8\ 39H_2O$; for oxalic acid, $(Al_2O_{2.92})_{100}(C_2O_4)_6(OH)_4\ 26H_2O$.

Surface morphology of porous anodic Al_2O_3 with different anode temperatures

SEM images of the surface morphology of the porous AAO films formed in the anode temperature range of 10–60 °C are shown in Fig. 5.

The SEM data show d_{pore} and D_{inter} values of 12.5 ± 0.1 nm and 52.5 ± 0.2 nm, respectively, which were found to be independent of anode temperature in the range from 10 to 40 °C. When the anode temperature increased from 50 to 60 °C, a decrease in the interpore distance from

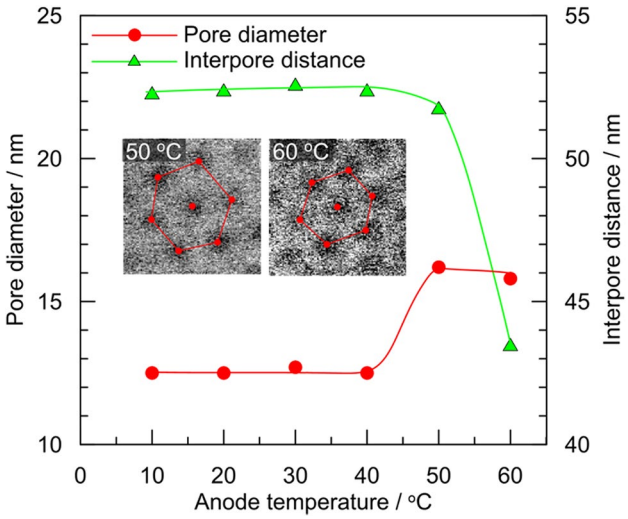

Fig. 6 Variation in the average pore diameter and average interpore distance of self-ordered anodic alumina obtained by anodization in 1.0 M sulfuric acid (20 °C) at 20 V as a function of anode temperature

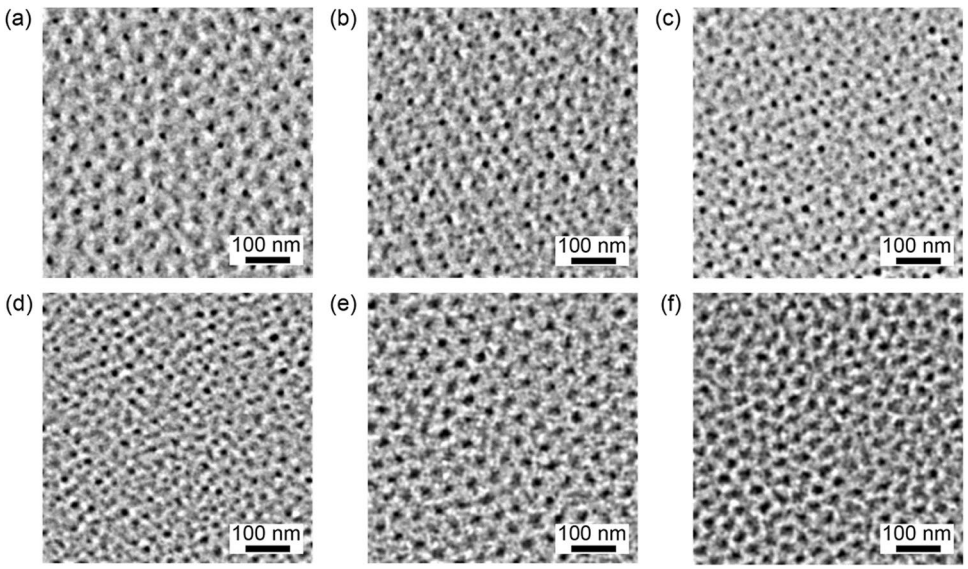

Fig. 5 SEM images of surface morphology of self-ordering of anodic alumina formed at different anode temperatures of (a) 10 °C, (b) 20 °C, (c) 30 °C, (d) 40 °C, (e) 50 °C, and (f) 60 °C at 20 V, in 1.0 M sulfuric acid solution (20 °C)

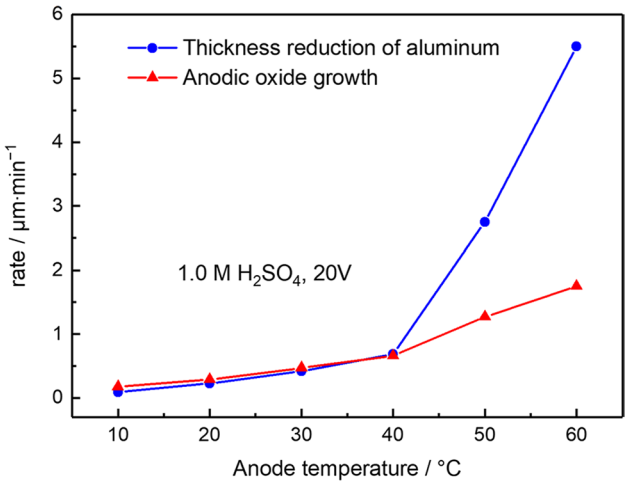

Fig. 7 Change in the thickness reduction rate of aluminum and in the rate of anodic aluminum oxide growth with anode temperature

51.8 nm (50 °C) to 43.5 nm (60 °C) was observed (Fig. 6). In this case, the pore diameter increased from 12.5 nm (40 °C) to 16.2 and 15.8 nm (50 and 60 °C, respectively).

It is important to consider the nature of the change in the proportionality coefficient (D_{inter}/U) for anodic films with anode temperatures of 50 and 60 °C. Data from the analysis show that the value of the proportionality coefficient (D_{inter}/U) decreases from 2.59 to 2.18 when the anode temperature increases from 50 to 60 °C. In accordance with [25], this indicates a decrease in mechanical stress in the anodic oxide film with an anode temperature of 60 °C. In turn, a decrease in mechanical stress should lead to an increase in the porosity of the AAO film in order to maintain a balance in the stress–strain state of the Al–Al_2O_3 system. The changes in the pore diameter are plotted in Fig. 6 to confirm this result.

Figure 7 presents a graph showing the rate of thickness reduction of aluminum (according to Fig. 1; the duration of anodization corresponds to the plateau stage of anodic current) and the rate of AAO (AAO) growth (according to Fig. 1; the duration of Al_2O_3 formation corresponds to the stage of anodic current until it completely declines) as a function of anode temperature. The behavior of the two lines is in good agreement up to a temperature of 40 °C. However, at higher temperatures, a dramatic divergence in their behavior is observed, which may be due to chemical dissolution.

As can be seen from the graph in Fig. 7, the thickness reduction rate for aluminum is clearly divided into two different stages. As the anode temperature increases from 20 to 40 °C, a gradual increase in the thickness reduction rate for aluminum is observed (first stage), while the porous structure of the formed anodic films remains unchanged. When the anode temperature increases above 40 °C, a sharp increase in the rate of thickness reduction is observed (second stage), which is accompanied by a change in the porous structure of the anodic films (Fig. 6). The data for the first stage show that by increasing the temperature of the anode, it is possible to increase the rate of ionic transfer in AAO, achieving a greater than threefold increase in the rate of AAO growth with an increase in temperature from 20 to 40 °C, without altering the porosity morphology of the anodic films.

Conclusions

The growth kinetics and surface morphology of AAO were studied for anodization processes in 1 M H_2SO_4 at different anode temperatures. To determine the ionic conductivity as a function of temperature, it was proposed to consider that ionic conductivity is directly proportional to ionic current. A plot of ionic conductivity versus anode (aluminum) temperature in Arrhenius coordinates exhibited a straight line. According to the results, the activation energy of ionic conductivity of AAO for sulfuric acid was 0.41 eV, which was greater than that of 0.34 eV for oxalic acid. The higher activation energy for sulfuric acid in this case was explained by a large deviation from stoichiometry for AAO due to the introduction of anionic impurities in the electrolyte.

The effect of anode temperature on the pore diameter (d_{pore}) and the interpore distance (D_{inter}) was also investigated. It was demonstrated that in the temperature range from 10 to 40 °C, the d_{pore} and D_{inter} did not change with anode temperature, exhibiting values equal to 12.5 ± 0.1 nm and 52.5 ± 0.2 nm, respectively. When the anode temperature (aluminum) increased to 60 °C, d_{pore} increased to 16 nm.

These results show that by increasing the temperature of the anode (aluminum) from 20 to 40 °C, it is possible to increase the ionic conductivity of AAO and thus achieve a greater than threefold increase in the rate of AAO growth, without altering the porous morphology of the anodic films.

Acknowledgements I. Vrublevsky and N. Lushpa acknowledge the support provided by the Belarusian Republican Foundation for Fundamental Research (Grant No. F23RNF-160).

Funding Belarusian Republican Foundation for Fundamental Research,F23RNF-160,Igor Vrublevsky,F23RNF-160,Nikita Lushpa

References

1. Eessaa AK, El-Shamy AM (2023) Review on fabrication, characterization, and applications of porous anodic aluminum oxide films with tunable pore sizes for emerging technologies. Microelectron Eng 279:112061. https://doi.org/10.1016/j.mee.2023.112061
2. Ku CA, Yu CY, Hung CW, Chung CK (2023) Advances in the Fabrication of Nanoporous Anodic Aluminum Oxide and Its Applications

to Sensors: A Review. Nanomaterials 13:2853. https://doi.org/10.3390/nano13212853
3. Domagalski JT, Xifre-Perez E, Marsal LF (2021) Recent advances in nanoporous anodic alumina: Principles, engineering, and applications. Nanomaterials 11:430. https://doi.org/10.3390/nano11020430
4. Law CS, Lim SY, Abell AD et al (2018) Nanoporous anodic alumina photonic crystals for optical chemo-and biosensing: Fundamentals, advances, and perspectives. Nanomaterials 8:788. https://doi.org/10.3390/nano8100788
5. Shingubara S (2003) Fabrication of nanomaterials using porous alumina templates. J Nanoparticle Res 5:17–30. https://doi.org/10.1023/A:1024479827507
6. Lee W, Park SJ (2014) Porous anodic aluminum oxide: Anodization and templated synthesis of functional nanostructures. Chem Rev 114:7487–7556. https://doi.org/10.1021/cr500002z
7. Sulka GD, Stepniowski WJ (2009) Structural features of self-organized nanopore arrays formed by anodization of aluminum in oxalic acid at relatively high temperatures. Electrochim Acta 54:3683–3691. https://doi.org/10.1016/j.electacta.2009.01.046
8. Ono S, Saito M, Ishiguro M, Asoh H (2004) Controlling Factor of Self-Ordering of Anodic Porous Alumina. J Electrochem Soc 151:B473–B478. https://doi.org/10.1149/1.1767838
9. Chernyakova K, Vrublevsky I, Klimas V, Jagminas A (2018) Effect of Joule Heating on Formation of Porous Structure of Thin Oxalic Acid Anodic Alumina Films. J Electrochem Soc 165:E289–E293. https://doi.org/10.1149/2.1001807jes
10. Ono S, Masuko N (2003) Evaluation of pore diameter of anodic porous films formed on aluminum. Surf Coatings Technol 169–170:139–142. https://doi.org/10.1016/S0257-8972(03)00197-X
11. Zaraska L, Stępniowski WJ, Ciepiela E, Sulka GD (2013) The effect of anodizing temperature on structural features and hexagonal arrangement of nanopores in alumina synthesized by two-step anodizing in oxalic acid. Thin Solid Films 534:155–161. https://doi.org/10.1016/j.tsf.2013.02.056
12. Leontiev AP, Roslyakov IV, Napolskii KS (2019) Complex influence of temperature on oxalic acid anodizing of aluminium. Electrochim Acta 319:88–94. https://doi.org/10.1016/j.electacta.2019.06.111
13. Aerts T, Jorcin JB, De Graeve I, Terryn H (2010) Comparison between the influence of applied electrode and electrolyte temperatures on porous anodizing of aluminium. Electrochim Acta 55:3957–3965. https://doi.org/10.1016/j.electacta.2010.02.044
14. Aerts T, Dimogerontakis T, De Graeve I et al (2007) Influence of the anodizing temperature on the porosity and the mechanical properties of the porous anodic oxide film. Surf Coatings Technol 201:7310–7317. https://doi.org/10.1016/j.surfcoat.2007.01.044
15. Li J, Wei H, Zhao K et al (2020) Effect of anodizing temperature and organic acid addition on the structure and corrosion resistance of anodic aluminum oxide films. Thin Solid Films 713:138359. https://doi.org/10.1016/j.tsf.2020.138359
16. Białek E, Włodarski M, Norek M (2020) Influence of anodization temperature on geometrical and optical properties of porous anodic alumina(PAA)-Based photonic structures. Materials (Basel) 13:3185. https://doi.org/10.3390/ma13143185
17. Sulka GD, Parkoła KG (2007) Temperature influence on well-ordered nanopore structures grown by anodization of aluminium in sulphuric acid. Electrochim Acta 52:1880–1888. https://doi.org/10.1016/j.electacta.2006.07.053
18. Ayalew AA, Han X, Sakairi M (2024) Effect of substrate temperature and electrolyte composition on the fabrication of through-hole porous AAO membrane with SF-MDC. Mater Chem Phys 323:129658. https://doi.org/10.1016/j.matchemphys.2024.129658
19. Aerts T, De Graeve I, Terryn H (2009) Control of the electrode temperature for electrochemical studies: A new approach illustrated on porous anodizing of aluminium. Electrochem commun 11:2292–2295. https://doi.org/10.1016/j.elecom.2009.10.013
20. Chernyakova K, Tzaneva B, Vrublevsky I, Videkov V (2020) Effect of Aluminum Anode Temperature on Growth Rate and Structure of Nanoporous Anodic Alumina. J Electrochem Soc 167:103506. https://doi.org/10.1149/1945-7111/ab9d65
21. Chernyakova K, Videkov V, Tzaneva B, Vrublevsky I (2019) *Monitoring of electrode temperature in exothermic electrochemical process*. In: 2019 28th International Scientific Conference Electronics, ET 2019 - Proceedings. https://doi.org/10.1109/ET.2019.8878579
22. Lee J, Kim Y, Jung U, Chung W (2013) Thermal conductivity of anodized aluminum oxide layer: The effect of electrolyte and temperature. Mater Chem Phys 141:680–685. https://doi.org/10.1016/j.matchemphys.2013.05.058
23. Vera-Londono L, Ruiz-Clavijo A, Caballero-Calero O, Martín-González M (2020) Understanding the thermal conductivity variations in nanoporous anodic aluminum oxide. Nanoscale Adv 2:4591–4603. https://doi.org/10.1039/d0na00578a
24. Darling HE (1964) Conductivity of Sulfuric Acid Solutions. J Chem Eng Data 9:421–426. https://doi.org/10.1021/je60022a041
25. Chernyakova K, Vrublevsky I, Jagminas A, Klimas V (2021) Effect of anodic oxygen evolution on cell morphology of sulfuric acid anodic alumina films. J Solid State Electrochem 25:1453–1460. https://doi.org/10.1007/s10008-021-04925-x
26. Crossland AC, Habazaki H, Shimizu K et al (1999) Residual flaws due to formation of oxygen bubbles in anodic alumina. Corros Sci 41:1945–1954. https://doi.org/10.1016/S0010-938X(99)00035-9
27. Shimizu K, Habazaki H, Skeldon P et al (2002) Role of metal ion impurities in generation of oxygen gas within anodic alumina. Electrochim Acta 47:1225–1228. https://doi.org/10.1016/S0013-4686(01)00836-2
28. Zhu XF, Li DD, Song Y, Xiao YH (2005) The study on oxygen bubbles of anodic alumina based on high purity aluminum. Mater Lett 59:3160–3163. https://doi.org/10.1016/j.matlet.2005.05.038
29. Torrescano-Alvarez JM, Curioni M, Skeldon P (2017) Gravimetric Measurement of Oxygen Evolution during Anodizing of Aluminum Alloys. J Electrochem Soc 164:C728–C734. https://doi.org/10.1149/2.0371713jes
30. Stępniowski WJ, Bojar Z (2011) Synthesis of anodic aluminum oxide (AAO) at relatively high temperatures. Study of the influence of anodization conditions on the alumina structural features. Surf Coatings Technol 206:265–272. https://doi.org/10.1016/j.surfcoat.2011.07.020
31. Du P, Zhu H, Braun A et al (2024) Entropy and Isokinetic Temperature in Fast Ion Transport. Adv Sci 11:2305065. https://doi.org/10.1002/advs.202305065
32. Tamburrano A, De Vivo B, Höijer M et al (2011) Effect of electric field polarization and temperature on the effective permittivity and conductivity of porous anodic aluminium oxide membranes. Microelectron Eng 88:3338–3346. https://doi.org/10.1016/j.mee.2011.08.007
33. Thompson GE, Wood GC (1983) Anodic Films on Aluminium 23:205–329. https://doi.org/10.1016/B978-0-12-633670-2.50010-3
34. Mata-Zamora ME, Saniger JM (2005) Thermal evolution of porous anodic aluminas: A comparative study. Rev Mex Fis 51:502–509